
RISK MARKERS BY SEX AND AGE GROUP FOR IN-HOSPITAL MORTALITY IN PATIENTS WITH STEMI OR NSTEMI: AN APPROACH BASED ON MACHINE LEARNING

A PREPRINT

Blanca Vázquez¹, Gibran Fuentes¹, Fabian Garcia¹, Gabriela Borrero², and Juan Prohias³

¹Instituto de Investigaciones en Matemáticas Aplicadas y en Sistemas, Mexico City, Mexico.

²Centro Médico, Nacional, Siglo XXI, Instituto Mexicano del Seguro Social, Mexico City, Mexico.

³Cardiocentro, Hospital Clínico - Quirúrgico Hermanos Ameijeiras, La Habana, Cuba.

December 23, 2024

ABSTRACT

Machine learning (ML) has demonstrated promising results in the identification of clinical markers for Acute Coronary Syndrome (ACS) from electronic health records (EHR). In the past, the ACS was perceived as a health problem mainly for men and women were under-represented in clinical trials, which led to both sexes receiving the same clinical attention. Although some approaches have emphasized the importance of distinguishing markers, these distinctions remain unclear. This study aims at exploiting ML methods for identifying in-hospital mortality markers by sex and age-group for patients with ST-elevation myocardial infarction (STEMI) and the Non-ST-elevation myocardial infarction (NSTEMI) from EHR. From the MIMIC-III database, we extracted 1,299 patients with STEMI and 2,820 patients with NSTEMI. We trained and validated mortality prediction models with different hyperparameters, clinical sets, and ML methods. Using the best performing model and a game-theoretic approach to interpret predictions, we identified risk markers for patients with STEMI and NSTEMI separately. The models based on Extreme Gradient Boosting achieved the highest performance: AUC=0.92 (95% CI:0.87-0.98) for STEMI and AUC=0.87 (95% CI:0.80-0.93) for NSTEMI. For STEMI, the top markers for both sexes are the presence of hyponatremia, and metabolic acidosis. More specific markers for women are acute kidney failure, and age>75 years, while for men are chronic kidney failure, and age>70 years. In contrast, for NSTEMI, the top markers for both sexes are advanced age, and intubation procedures. The specific markers for women are low creatinine levels and age>60 years, whilst, for men are damage to the left atrium and age>70 years. We consider that distinguishing markers for sexes could lead to more appropriate treatment strategies, thus improving clinical outcomes.

Keywords STEMI · NSTEMI · Machine learning · In-hospital mortality prediction · Risk markers

1 Introduction

Acute Coronary Syndrome (ACS) is associated with the rupture of an atherosclerotic plaque inside the coronary artery and is a leading cause of mortality and disability worldwide[1]. The two most common ACS types are ST-elevation myocardial infarction (STEMI) and the Non-ST-elevation myocardial infarction (NSTEMI). In the past, the ACS was perceived as a health problem only for men; hence women were under-represented in the clinical trials [2]. This fact caused that both sexes received the same clinical attention [3]. However, some studies have highlighted the importance of distinguishing markers by sex and age because of the differences in biological and physiological characteristics [4]. For instance, Rodriguez et al. [5] reported the differences in in-hospital mortality by sex and identified that women have a higher risk of death after a STEMI and a lower risk of death after an NSTEMI. In contrast, Onose et al. [6] analyzed the sex differences after a natural disaster in cardiovascular patients and found that post-traumatic

stress disorder was more prevalent in women than in men. Other works analyzed the sex differences in readmission rates and complications[7], the opportunities to be resuscitated after a cardiac arrest [8], and guidelines of care for STEMI - NSTEMI and their association with 30-day and 3-year mortality [9]. Although these studies reveal important differences between sexes, specific clinical markers to assess the risk of mortality in each of these sub-populations for STEMI and NSTEMI have not been identified explicitly. Traditionally, the identification of risk markers for ACS has been done through retrospective and prospective studies. The results of these studies have enabled the development of scoring systems, such as TIMI [10], PURSUIT [11] and GRACE [12], that estimate the risk of mortality for ACS patients from a set of relevant clinical markers. However, several studies have pointed out disadvantages that limit the effectiveness of these scoring systems. For instance, they are usually calculated by hand using limited clinical features characterized by abnormal observations, require features that are not always readily available (e.g., the Killip class), and they do not distinguish markers by sub-populations of patients [13, 14].

During in the last decade, machine learning models that leverage electronic health records (EHR) have demonstrated promising results in accelerating the identification of markers and the development of auxiliary tools to make clinical decisions [15]. For instance, Austin et al. [16] trained ensemble-based methods with results of laboratory, vital signs and physical examination data to predict the probability of 30-day mortality in patients with cardiovascular diseases; they found that the age, systolic blood pressure, glucose, creatinine and heart rate increase the risk of mortality. Similarly, McNamara et al. [17] used logistic regression with medical history, initial laboratory values and vital signs for predicting in-hospital mortality in patients with myocardial infarction. They identified the age, heart rate, systolic blood pressure, creatinine, troponin, cardiac arrest, cardiogenic shock, and heart failure as risk markers. On the other hand, Chen et al. [18] carried out a multivariate regression analysis of in-hospital mortality in patients over 80 years old using demographic data, medical history, hemodynamic and laboratory measurements. The associated mortality predictors in this study were: history of stroke, cardiac shock, Killip class III to IV, pulse rate, ejection fraction, ventricular tachycardia, serum creatinine concentration, and elevated initial white blood cells.

However, to the best of our knowledge, risk markers by sex and age-group for STEMI and NSTEMI have not been identified separately. This work aims to exploit in-hospital mortality prediction models based on machine learning together with a game-theoretic approach to model interpretation for identifying the markers in each of the desired sub-populations.

2 Methods

2.1 Study population

In this study, we used the MIMIC-III database [19], which is a publicly and freely available dataset characterized by ICU patients with diverse conditions of the Beth Israel Deaconess Medical Center between 2001 and 2012. From MIMIC-III, we extracted EHRs using the codes 410.00-411.1 for STEMI and 410.70-410.72 for NSTEMI, as defined by the International Classification of Diseases, Ninth Revision (ICD-9)[20]. In Additional file 1, we describe the codes in detail. Our cohorts consist of 1,299 patients diagnosed with STEMI and 2,820 with NSTEMI with a length of stay longer than 24 hours. Overall, for STEMI, the median age of the patients was 67.26 ± 13.86 years, and 65% were male. In contrast, for NSTEMI, the patient's median age was 72.29 ± 13.38 years, and 58% were male. Additionally, the mortality rate for STEMI was 6.77% and 9.21% for NSTEMI. Table 1 shows a summary of the statistics for each cohort.

In Figure 1, we showed the overall process used for identifying risk markers for each sub-population. This process includes the extraction and pre-processing of EHRs, training and evaluating machine learning models, and identifying and validating risk markers. This is a common process for building and evaluating machine learning models, widely used in cardiovascular research [21].

2.2 Data extraction

In Table 2, we described the static and dynamic clinical features extracted for each cohort. The static features were demographics data, and the dynamic features were laboratory results, vital signs, blood gas, ventilation data, hemodynamic, complications, treatments, and procedures. We represented the static features and some dynamic features, such as complications, treatments, and procedures using one-hot encoding. We used a representation of minimum, maximum, and average values for the rest of the dynamic features as commonly done in the literature [14]. It is worth noting that some features did not exist in MIMIC-III database for STEMI compared with NSTEMI, such as precordial leads. Consequently, we extracted a total of 191 features for STEMI and 201 for NSTEMI.

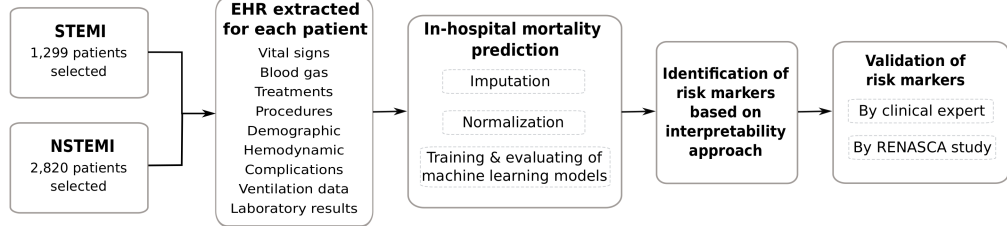


Figure 1: Process for identifying risk markers by sex and age-group for STEMI and NSTEMI patients using machine learning methods

Table 1: Statistics of the cohorts of patients

Feature	STEMI				NSTEMI			
	Total cohort n=1299	Women n=460 (35%)	Men n=839 (65%)	P-value	Total cohort n=2820	Women n=1176 (42%)	Men n=1644 (58%)	P-value
Age	67.26±13.86	72.89±13.33	64.17±13.16	<0.001	72.29±13.38	74.40±12.50	70.66±12.60	<0.001
Weight (kg)	79.65±17.83	72.02±15.83	86.19±16.58	0.325	81.18±17.67	72.92±16.90	84.46±16.89	0.019
Risk factors								
Hypertension	647 (49.80%)	228 (49.56%)	419 (49.94%)	0.284	1,313 (46.56%)	585 (49.74%)	728 (44.28%)	0.3
Diabetes	292 (22.47%)	103 (22.39%)	189 (22.52%)	0.097	800 (28.36%)	331 (28.14%)	469 (28.52%)	0.015
Smoking	170 (13.08%)	43 (9.34%)	127 (15.13%)	0.006	198 (7.02%)	69 (5.86%)	129 (7.84%)	<0.001
Hemodynamic assessment								
Heart rate (bpm)	80.81±14.33	82.08±14.38	80.11±14.25	<0.001	83.72±14.09	84.13±14.47	83.42±13.79	<0.001
Respiration rate (bpm)	19.57±8.98	20.56±11.23	19.17±7.84	0.1	19.06±3.89	19.26±4.06	18.91±3.75	<0.001
SysBP (mmHg)	112.09±14.35	112.21±14.38	112.27±13.92	<0.001	116.25±15.53	117.37±16.48	115.44±14.75	<0.001
DiasBP (mmHg)	61.00±9.64	57.20±8.72	63.06±9.50	0.004	57.62±11.02	56.02±9.93	58.77±11.59	0.009
Biochemistry determinations								
HbA1c (g/dl)	6.56±0.76	6.55±0.58	6.56±0.83	0.778	6.73±0.52	6.72±0.49	6.72±0.53	<0.001
Creatinine (µmol/L)	3.23±10.94	3.32±9.48	3.17±11.66	<0.001	5.58±12.77	4.80±10.38	6.14±14.21	<0.001
CK-MB (U/L)	197.37±212.11	184.70±195.37	204.39±220.5	<0.001	52.57±71.20	47.39±59.98	56.28±78.03	<0.001
Troponin T	8.31±12.05	8.19±9.18	8.37±13.38	0.08	3.04±7.10	3.07±8.82	3.01±5.54	0.012
Complications								
Atrial fibrillation	323 (24.86%)	129 (28.04%)	194 (23.12%)	<0.001	962 (34.11%)	397 (33.75%)	565 (34.36%)	0.08
Acute renal failure	159 (12.24%)	64 (13.91%)	95 (11.32%)	<0.001	760 (26.95%)	317 (26.95%)	443 (26.94%)	<0.001
RBBB	100 (7.69%)	42 (9.13%)	58 (6.91%)	0.867	256 (9.70%)	100 (8.50%)	156 (9.48%)	0.038
LBBB	60 (4.6%)	18 (3.91%)	42 (5.0%)	<0.001	254 (9.0%)	105 (8.92%)	149 (9.06%)	0.076
Treatments								
ACE inhibitors	360 (27.71%)	103 (22.39%)	257 (30.63%)	<0.001	329 (11.66%)	134 (11.39%)	195 (11.86%)	<0.001
Diuretics	341 (15.50%)	130 (28.26%)	211 (25.14%)	0.418	1094 (38.78%)	456 (38.77%)	638 (38.87%)	0.003
Aspirin	224 (17.24%)	79 (17.17%)	145 (17.28%)	0.05	744 (26.38%)	292 (24.82%)	452 (27.49%)	0.116
Clopidogrel	152 (11.70%)	50 (10.86%)	102 (12.15%)	0.362	286 (10.14%)	112 (9.52%)	174 (10.58%)	<0.001
Average stay (days)	4.39	4.57	4.30		5.12	5.26	5.02	
Number of patients expired (first 24 hours)	88 (6.77%)	42 (9.13%)	46 (5.48%)		260 (9.21%)	126 (10.71%)	134 (8.15%)	<0.001

Note: ACE inhibitors, Angiotensin-converting enzyme inhibitors; bpm, beats per minute; bpm, breaths per minute; CK-MB, Creatinine kinase MB fraction; DiasBP, Diastolic blood pressure; g/dl, grams per deciliter; HbA1c, glycated haemoglobin; LBBB, Left bundle branch block; mmHg, millimeters of mercury; RBBB, Right bundle branch block; SysBP, Systolic blood pressure; U/L, unit per liter; µmol/L, micromol per liter. Data shows are mean ± standard deviation for continuous features and as percentage for categorical features

2.3 In-hospital mortality prediction models

First, missing values of the EHR dataset were filled with the mean from all the observable values. We pay special attention to features that have shown to be associated with myocardial infarction size and heart injuries (e.g., troponins, pulmonary artery pressure, and leads). The values of these features were gathered from the clinical notes using a set of regular expressions. We also performed feature-wise normalization on each sample by subtracting the mean and dividing by the standard deviation. Finally, the resulting data set was split randomly into non-overlapping training and test sets consisting of 80% and 20%.

Then, we trained and evaluated state-of-art methods commonly used in clinical trials for the prediction of specific events, namely Logistic Regression (LR), Support Vector Machines (SVM), Random Forest (RF), and eXtreme Gradient Boosting (XGB). For each method, we used grid search for hyperparameter selection based on prediction performance. For LR, we used the *saga* optimizer and considered ℓ_1 , ℓ_2 , and *elasticnet* norms for weight penalization. Similarly, for SVM, we explored the ℓ_1 and ℓ_2 weight penalization norms. For both SVM and LR, we explore different strengths C of penalization on a logarithmic scale in a range from -3 to 3 .

For RF, the base-2 logarithm of the available features was used as the maximum number of features for each split and the quality of the split was measured by the *gini* function. For XGB, ℓ_1 and ℓ_2 norms for weight penalization and

Table 2: Clinical features extracted for each cohort. Each clinical set was used to train machine learning models.

Clinical set	Features
Demographic information	gender, age, admission type (elective, emergency, urgent), status (divorced, married, single, widow), weight admit
Complications	rbbb, lbbb, av block, atrial fibrillation, ventricular fibrillation, ventricular tachycardia, cardiogenic shock, mitral regurgitation, pericarditis, renal failure, angina, cerebrovascular accident, cardiac arrest, congestive heart failure, chronic airway obstruction, hypertension, aneurysm, diabetes, tobacco, alcohol abuse, leads (i,ii,iii,v1,v2, v3, v4, v5, v6, avf, avr, avl, f) Also for STEMI: leads (v1r, v2r), qtc wave Also for NSTEMI: leads (lv, l, v), septal rupture, anterolateral, precordial, inferolateral, anterior, lateral, mid lateral, posterolateral, inferior, waves (r, qt, inverted t, qrs, rv), left ventricular hypertrophy
Treatments	aspirin, clopidogrel bisulfate, enoxaparin, heparin, oral nitrates statins, fibrates, beta blockers, ace inhibitors, arb, diuretics, calcium antagonist, amiodarone, digoxin, dobutamine, dopamine, oral glucose low drugs, insulin, potassium chloride, warfarin, vancomycin
Procedures	coronary arteriography using two catheters, injection or infusion of platelet inhibitor, combined right and left heart cardiac catheterization, replacement of tracheostomy tube, angiocardiography of left heart structures, insertion of endotracheal tube, extracorporeal circulation auxiliary to open-heart surgery, implant of pulsation balloon, venous catheterization, angiocardiography of right heart structures, coronary arteriography using a single catheter, arterial catheterization, insertion of temporary transvenous pacemaker system
Blood gas during ICU stay	alveolar arterial gradient, base excess, so2, ph, totaleco2, chloride, calcium, lactate, fio2, pco2, po2, bicarbonate
Laboratory results	anion gap, albumin, bands, creatinine, protein creatinine ratio, fibrinogen, uric acid, triglycerides, positive end expiratory pressure, eosinophils, neutrophils, lymphocytes, basophils, monocytes, cholesterol (total, hdl, ldl), hemoglobin a1c, platelet, potassium, partial thromboplastin time, international normalized ratio, prothrombin time, sodium, urea, white blood cells, hematocrit, hemoglobin, troponin i, troponin t, glucose, creatine, creatine kinase ck, creatine kinase mb
Hemodynamic	cardiac out, intracranial pressure, pulmonary artery pressure (systolic, diastolic, mean), central venous pressure, ventricular assist device (left, right), pulmonary capillary wedge pressure, mixed venous oxygen saturation, pulmonary artery line, ventricular assist devices beat rate (left, right),
Vital signs	heart rate, blood pressure (systolic, diastolic, mean), respiratory rate, oxygen saturation, temperature

0.05, 0.1, and 0.5. for the learning rate were considered. We used 0.3, 0.4, 0.8, and 0.9 as subsample ratio to randomly sample the training data prior to growing the trees. Also, we examined 0.3 and 0.5 for dropout rate and values 10–50 for γ . Models with 50, 100, and 200 trees with a maximum depth of 2, 4, and 6 nodes were evaluated for both RF and XGB.

For all methods, we used weighted loss functions to mitigate the class imbalance. Specifically, the loss for the class c is weighted by

$$w_c = \frac{n}{2 \cdot n_c} \quad (1)$$

where w_c is the weight of the class $c \in \{0, 1\}$, n is the total of samples in the dataset, and n_c is the number of samples for class c .

We performed a grid-search with 10 repetitions of 5-fold cross-validation to assess all the possible combinations of hyperparameters for each method. We trained a method with each extracted clinical set and also a method with the combination of all clinical sets. We used the AUC (Area Under The Curve) ROC (Receiver Operating Characteristics)

curve to measure model performance and the AUC score to measure true positive rate vs. false positive rate, which is commonly used for imbalanced classification tasks. As result, we identified the hyperparameters and selected the model that produces the highest cross-validated mean AUC for each cohort. We used the test set to measure the performance of models. For implementation, we used scikit-learn [22] for LR, SVM, and RF, and XGBoost [23] for XGB. The source code of our implementation is available at https://github.com/blancavazquez/Riskmarkers_ACS.

For comparing the performance of prediction models implemented, we calculated the GRACE score, which is the most common clinical score for predicting mortality for ACS. This score uses eight markers to predict mortality: age, heart rate, systolic blood pressure, creatinine, cardiac arrest, ST-segment deviation, cardiac enzymes, and Killip class. We extracted the values for all these markers, calculated the points using the GRACE scale[24], and computed the ROC-curve and AUC score for each cohort.

2.4 Identification of risk markers for STEMI and NSTEMI patients

We selected the model with the best performance for each cohort and used an interpretability approach to identify risk markers. Our goal is to explain how each clinical feature contributes to increasing the mortality in patients with STEMI and NSTEMI. To do this, we used the SHapley Additive exPlanations (SHAP) approach [25] for interpreting the output of the model through computing the contribution of each feature. This approach has been recently used to interpret machine learning models for identifying markers for chronic kidney disease [26] and hypoxaemia risk [27].

The SHAP approach is based on Shapley values[28] from game theory, where the game is the prediction task for a single instance, and the players are the values of the features. Overall, this approach computes the contribution that each player leads to the game. The Shapley value is the average marginal contribution of that feature across all possible combinations of features:

$$\phi_j(val) = \sum_{S \subseteq \{x_1, \dots, x_p\} \setminus \{x_j\}} \frac{|S|!(p - |S| - 1)!}{p!} (val(S \cup \{x_j\}) - val(S)) \quad (2)$$

where S is a subset of features used in the prediction task, p is the total number of features, x is the vector of feature values to be interpreted, and $val(S)$ is the prediction for feature values in set S that are marginalized over features that are not in set S . The SHAP approach computed Shapley values from coalitional game theory; hence, we used SHAP to compute the contribution of each feature to the mortality prediction.

One advantage of SHAP is that it allows calculation and plot of the SHAP feature importance, SHAP summary, SHAP interactions, and SHAP explanation force to compute the contribution of each feature. The SHAP feature importance is computed by averaging the absolute Shapley values per feature across the data (see equation 3). Hence, the features with large absolute Shapley values are important features for the prediction task. Overall, the SHAP feature importance plot shows the global importance of the features arranged in order of importance.

$$I_j = \sum_{i=1}^n |\phi_j^{(i)}| \quad (3)$$

Likewise, the SHAP summary shows the distribution of Shapley values of the features over all instances. Thus, this plot shows two main results: the most important features that impact the prediction and the feature value (low - high) that increase or decrease the prediction. On the other hand, SHAP interactions compute the Shapley interactions values for all features obtained a matrix per instance of $n \times n$, where n is the number of features. For visualizing the interactions, a SHAP dependence plot is used. This plot visualizes a single feature where the x-axis shows the feature values, and the y-axis shows their Shapley value. Moreover, this plot uses the obtained matrix to identify the feature with the strongest interactions with the picked feature. Overall, SHAP interaction values are a generalization of SHAP values. Finally, the SHAP explanation force plot uses the marginal contribution of Shapley values to explain individual predictions. In this plot, we can visualize three elements: 1) the values of the features that contribute to an increase or decrease in the model's output value, 2) the output from the average value over all patients (base value), and 3) the SHAP values as arrows that push the output to the left or the right from the base value to increase or decrease the mortality risk.

We used the SHAP algorithm [29] for computing the Shapley values and identifying the risk markers for each sub-population.

2.5 Validation of risk markers

A set of expert cardiologists evaluated the reliability and utility of identified markers. This validation consists in determining whether these markers are useful for predicting mortality in routine clinical practice. Additionally, we compared the identified markers with a longitudinal-cohort study for STEMI and NSTEMI patients, called RENASCA[30], the first real-world study describing the features that contribute to mortality in both populations.

2.6 Statistical analysis

In Table 1, we reported the continuous features as mean \pm standard deviation and compared them with the T student test. Categorical features are expressed as percentages and compared using the chi-square test. We measured the performance of all models using the Area under the ROC Curve. We used the Delong test to compare the ROC curves of machine learning models and the GRACE score. We used the McNemar test to compare the proportion of errors between the machine learning models and GRACE on test sets; hence when the proportion of errors is different, the test suggests that there is a statistically significant difference between the model and GRACE ($p<0.05$). We used multivariable Cox regression to identify the statistically significant markers, and then these were compared with the markers identified by SHAP values.

3 Results

3.1 Performance of in-hospital mortality prediction models

In Table 3, we present a summary of the models with the top cross-validated mean AUC for all the clinical sets evaluated. Overall, XGB models obtained the best performances regardless of the clinical features used for training, followed by logistic regression and support vector machine models. We found that models trained with all the EHR extracted (called combined set) achieved higher performance than models trained with a single set (e.g., procedures or complications). Particularly, XGB-based models achieved the best AUC score of 0.90 for STEMI and 0.87 for NSTEMI using all EHR extracted on the test set.

For STEMI, the best hyperparameters obtained by cross-validation that produced the highest performance for the XGB model using the combined set were: number of trees = 100, a subsample ratio of 0.3, and the minimum loss reduction of 10. In contrast, for NSTEMI, the best hyperparameters for the XGB model were: number of trees = 250, a subsample ratio of 0.4, and the minimum loss reduction of 50. For both models, they matched in the number of subsample ratio of the training instances = 0.9, a maximum depth of 4, a learning rate of 0.1, a drop rate of 0.5, an alpha of 0.9, and lambda of 0.6.

In Figure 2, we show the AUC-ROC curves obtained by XGB models and by GRACE score. Overall, we identified that XGB models achieved a higher AUC score than GRACE. For STEMI (Figure 2, left-side), we visualize the performance of XGB model AUC=0.92 (95% CI:0.87-0.98), while GRACE achieved an AUC=0.64 (95% CI:0.36-0.66). In contrast, for NSTEMI (Figure 2, right-side), the XGB model achieved an AUC=0.87 (95% CI:0.80-0.93) and GRACE obtained an AUC=0.70 (95% CI:0.60-0.83). Moreover, for STEMI, the XGB model obtained a sensitivity of 0.94 and a specificity of 0.84, while GRACE obtained 0.88 and 0.42, respectively. For NSTEMI, the XGB model obtained a sensitivity of 0.92 and 0.76 of specificity, and GRACE achieved 0.1 and 0.89 for both metrics. In Additional Files 2 and 3, we present the performance of all the trained models for STEMI and NSTEMI, respectively.

3.2 Risk markers identified by sex and age-group for STEMI and NSTEMI

Figure 3 shows the top markers for predicting the risk of mortality ranked in descending order according to the feature importance for STEMI and NSTEMI using the SHAP summaries. In these summaries, we show how each of the markers and their values contributes to increase or decrease the risk. For example, the X-axis positive is associated with a high risk, and the X-axis negative is associated with a low risk for a feature. Likewise, the color indicates whether the value of the feature is high (red) or low (green) for that observation. For instance, in Figure 3a, we observed that high levels of urea, anion gap, heart rate, lactate, advanced age, potassium, and white blood cells (shown in red color) increase the risk mortality (X-axis positive) for STEMI. While the low levels of these markers (shown in green color) decrease the risk (X-axis negative). Besides, the markers that also increase the probability of death are cardiogenic shock, renal failure, and low levels of creatinine, systolic blood pressure, total CO₂, pH, sodium, and mean blood pressure.

In contrast, for NSTEMI (Figure 3d), we identified that long length of stay, advanced age, and high levels of urea, anion gap, lactate, heart rate, respiratory rate, and diastolic pap increase the risk of death. Similarly, procedures as

Table 3: Best performing models for predicting in-hospital mortality for STEMI and NSTEMI

Clinical set (No. features)	Model	STEMI AUC \pm std	NSTEMI AUC \pm std
Combined (191 STEMI, 201 NSTEMI)	LR	0.87 \pm 0.04	0.76 \pm 0.01
	RF	0.83 \pm 0.05	0.77 \pm 0.02
	SVM	0.84 \pm 0.04	0.83 \pm 0.02
	XGB	0.89 \pm 0.03	0.87 \pm 0.02
Laboratory results (40)	LR	0.83 \pm 0.04	0.75 \pm 0.03
	RF	0.79 \pm 0.04	0.68 \pm 0.03
	SVM	0.80 \pm 0.05	0.73 \pm 0.03
	XGB	0.87 \pm 0.03	0.76 \pm 0.02
Procedures (20)	LR	0.71 \pm 0.05	0.74 \pm 0.03
	RF	0.70 \pm 0.05	0.75 \pm 0.03
	SVM	0.72 \pm 0.05	0.76 \pm 0.02
	XGB	0.70 \pm 0.05	0.78 \pm 0.02
Complications (38 STEMI, 48 NSTEMI)	LR	0.81 \pm 0.05	0.75 \pm 0.03
	RF	0.69 \pm 0.09	0.69 \pm 0.04
	SVM	0.72 \pm 0.07	0.71 \pm 0.04
	XGB	0.80 \pm 0.05	0.74 \pm 0.03
Hemodynamic (28)	LR	0.60 \pm 0.05	0.60 \pm 0.03
	RF	0.54 \pm 0.07	0.59 \pm 0.03
	SVM	0.61 \pm 0.05	0.61 \pm 0.03
	XGB	0.62 \pm 0.05	0.64 \pm 0.03
Demographic (10)	LR	0.60 \pm 0.05	0.58 \pm 0.03
	RF	0.58 \pm 0.06	0.58 \pm 0.03
	SVM	0.61 \pm 0.06	0.60 \pm 0.03
	XGB	0.63 \pm 0.05	0.61 \pm 0.03
Treatments (21)	LR	0.72 \pm 0.05	0.63 \pm 0.04
	RF	0.65 \pm 0.07	0.62 \pm 0.04
	SVM	0.68 \pm 0.06	0.66 \pm 0.04
	XGB	0.71 \pm 0.06	0.67 \pm 0.04
Blood gas (14)	LR	0.73 \pm 0.06	0.67 \pm 0.04
	RF	0.66 \pm 0.08	0.70 \pm 0.03
	SVM	0.73 \pm 0.05	0.68 \pm 0.04
	XGB	0.78 \pm 0.06	0.75 \pm 0.03
Vital signs (20)	LR	0.71 \pm 0.07	0.69 \pm 0.04
	RF	0.62 \pm 0.07	0.63 \pm 0.04
	SVM	0.69 \pm 0.05	0.69 \pm 0.04
	XGB	0.70 \pm 0.06	0.72 \pm 0.03

Note: LR, Logistic Regression; SVM, Support Vector Machines; XGB, eXtreme Gradient Boosting; RF, Random Forest; 'combined' means to join all the clinical features extracted to train the model; std, standard deviation.

the insertion of an endotracheal tube and mechanical ventilation, complications as cardiogenic shock and low levels of creatinine, total CO₂, systolic blood pressure, temperature, and SpO₂ also increase the risk.

On the other hand, we identified the risk makers by sex and age-group using the SHAP feature importance. For instance, in Figure 3b, we identified that creatinine, urea, and anion gap are the most important markers that impact the risk of mortality for women with STEMI. In contrast, in Figure 3c, we identified that anion gap, urea, and heart rate are the most important markers that increase the risk for men with STEMI. Also, we found that troponin-T and mean blood pressure were identified only for women as predictors of death. Meanwhile, the identified markers exclusive for men were pulmonary artery pressure (pap) and lymphocytes. For NSTEMI, in Figure 3e and 3f, we identified that length of stay, insertion of an endotracheal tube, and age are markers that increase the risk for both sexes. In particular, women were associated with the markers of sodium, SpO₂, and diastolic blood pressure as predictors of death. Instead, men were related to the markers of diastolic pap, base excess, and lymphocytes.

In Figures 4 and 5, we show sex and age-specific differences and the interactions between markers for STEMI and NSTEMI. The X-axis corresponds to a marker, and the Y-axis shows the SHAP value assigned to such a marker. High SHAP values mean an increase in the mortality prediction, and different colors represent SHAP interaction values between markers. Each point corresponds to the prediction of a patient, and multiple points in the same location show

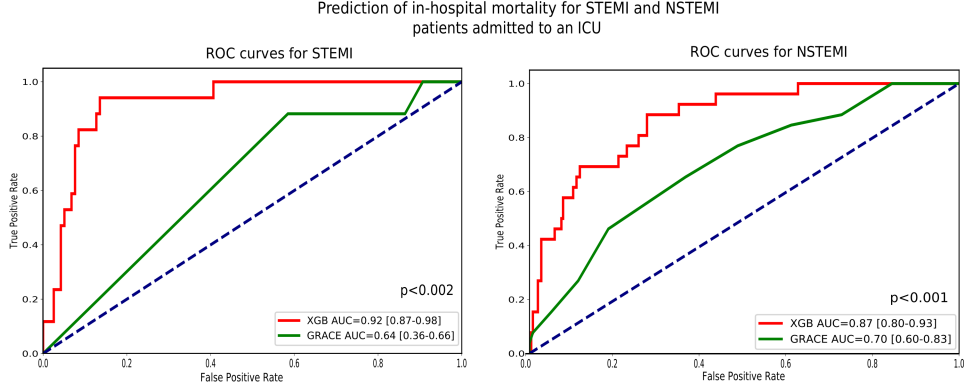


Figure 2: ROC curves for predicting in-hospital mortality within the first 24 hours of admission to an ICU after a STEMI (left) or NSTEMI (right). XGB-based models achieved higher AUCs than the GRACE score ($P<0.005$).

density. For instance, in Figure 4 at the top, we show the specific markers for women with STEMI and identify that the levels of urea >25 mg/dL increase the risk of death (positive SHAP values, Y-axis) when the creatinine levels are mostly below four umol/L. Instead, for men (Figure 4 at the bottom), we found that urea >20 mg/dL and the creatinine >6 umol/L increase the risk. Also, the level of creatinine >10 umol/L with levels of troponin-T >5 ng/L increases the risk for both sexes. Besides, for women, low levels of sodium <135 mEq/L with high values of ph >7.6 increase the risk of mortality. Additionally, sodium <135 mEq/L with ph >7.32 increase the risk for men. Overall, we observed that men over 70-year-old have a higher risk of dying than women over 75-year-old. Moreover, the men have a high risk of renal failure, high levels of creatinine kinase, and urea than women.

In contrast, for women with NSTEMI (Figure 5 at the top), the urea >20 mg/dL increases the risk of death with high creatinine >10 umol/L. Instead, for men (Figure 5 at the bottom), urea >25 mg/dL and creatinine >10 umol/L are markers that increment the risk. Also, low levels of creatinine (<20 umol/L) with troponin-T >3 ng/L are markers that increase women's risk. Similarly, for men, low levels of creatinine and troponin >2 increases the risk. Besides, for women, low levels of total CO₂ <25 mEq/L with a respiration rate >25 breaths per minute (bpm) indicate a high risk. While for men, the same result is with total CO₂ <23 mEq/L with a respiration rate >27.5 bpm. In general, women over 60 years have a higher risk than men whose risk is over 70 years. Particularly, we observed that women close to 60 years the level of urea is <40 mg/dL, white blood cells are <15 k/uL, and the length of stay is <6 days, while that women over 80 years, the levels of all these markers increased twice.

Figure 6 shows explanations of individual predictions for two patients with STEMI and two patients with NSTEMI. In Figure 6a, we observed the features of a patient diagnosed with STEMI who died in ICU. In this case, the model's output was a 'high risk of mortality' (base value=3.75 and output value=4.13). The features that increased the risk of this patient were high levels of partial thromboplastin time (89.07 seconds), urea (28 mg/dL), creatinine (14.2 umol/L), sodium (133.5 mEq/L), and renal failure (presence=1). In contrast, Figure 6b shows the individual prediction for a patient diagnosed with STEMI who survived. For this patient, the model outputted a low risk of mortality (output value=-0.43). The features that decreased the risk were normal levels of albumin (3.3 g/dL), and the absence of renal failure (presence=0) and mechanical ventilation (vent=0).

Instead, in Figure 6c, we can see a patient who died from NSTEMI for whom the model's output was a high risk of mortality (base value=2.83 and output value=3.82). For this patient, the features that increased the risk are the insertion of an endotracheal tube (presence=1), advanced age (86.62 years), and high levels of pap diastolic (27.15 mmHg). Finally, Figure 6d shows the explanations for a patient with NSTEMI who survived. In this case, the model's output was a low risk of mortality (output value=-2.71), and the features that decreased the risk were age (20.17 years), low levels of urea (6 mg/dL) and creatinine (0.5 umol/L), and no endotracheal tube (presence=0). Unlike patient C, the age and the absence of procedures contributed to the favorable outcome for this patient.

3.3 Clinical validation of the identified risk markers

We validated the identified markers in two manners. The first consisted of an assessment of the reliability and utility of markers by cardiologist experts. The second consisted of comparing our markers with those described in the RENASCA study.

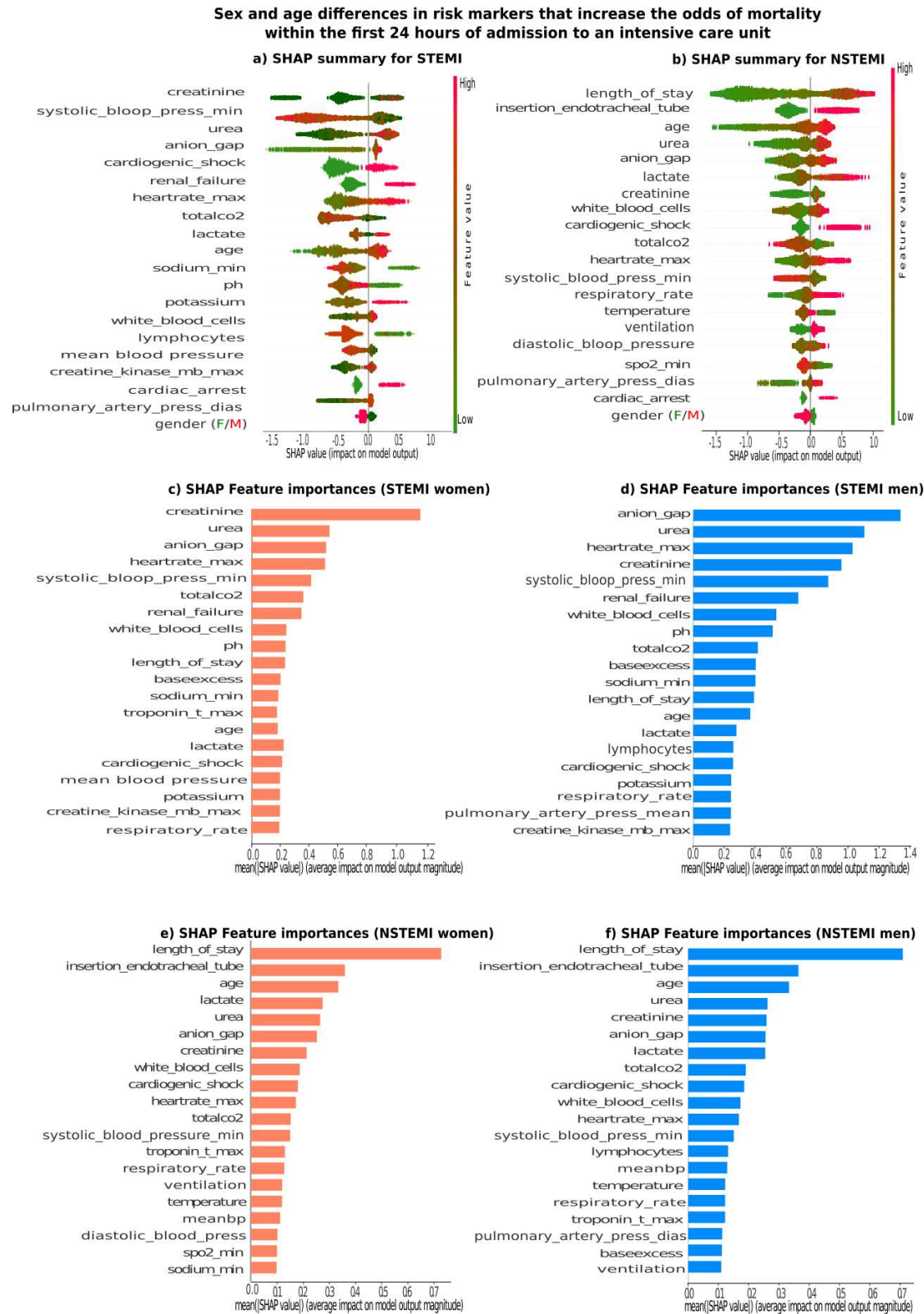


Figure 3: Risk markers that increase mortality within the first 24 hours of admission to the ICU according to sex and age-group for STEMI and NSTEMI based on the SHAP approach.

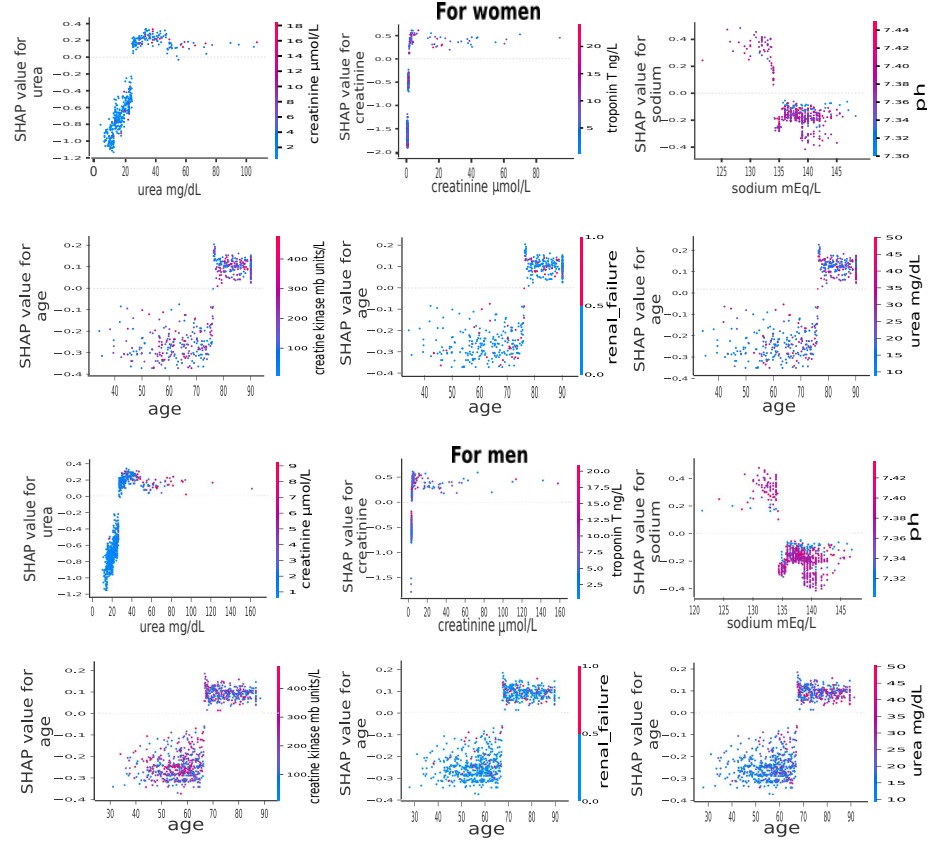


Figure 4: Sex and age-group differences in the top risk markers of patients with STEMI

Overall, the cardiologists concluded that the identified markers are coherent, comparable, and consistent with the clinical routine because they describe clinical trends well-established for patients with ACS. For instance, in the first evaluation, the cardiologists mentioned that the identification of markers according to sex and age is useful because they describe interesting clinical behaviors. Our approach identified that women with STEMI have a higher risk of mortality due to acute kidney failure (high urea levels with low levels of creatinine). While men with STEMI present chronic kidney failure (high levels of urea and creatinine).

Moreover, we identified that women with NSTEMI die younger than men (60 years versus 70), while that for STEMI, the men die younger than women (70 and 75 years, respectively). Besides, we identified that men with NSTEMI suffering from damage to the left atrium because, in this group, we found levels of diastolic pap. Also, we discovered that STEMI patients suffer from hyponatremia (low levels of sodium), tachycardia (high levels of heart rate), and metabolic acidosis (high levels of anion gap with low levels of ph, total CO₂, and sodium) compared to NSTEMI. Overall, for NSTEMI patients with an extended length of stay, advanced age, and an endotracheal tube insertion are lousy prognosis.

The second evaluation consisted of comparing the identified markers with the most common features described in the RENASCA study, which analyzed a large cohort of Mexican patients diagnosed with STEMI and NSTEMI enrolled in 177 different hospitals. We selected this study because it examines STEMI and NSTEMI separately for stratifying risk and identifying treatments. We found that the most common markers for STEMI in both studies were creatinine, urea, systolic blood pressure, heart rate, creatine kinase, troponin, and age. Correspondingly, for NSTEMI, the most common markers were metabolic acidosis, cardiogenic shock, respiratory rate, troponin, and the prevalence of advanced age women.

4 Discussion

In this approach, we exploited machine learning models based on EHR for identifying relevant clinical markers that increase the risk of mortality by sex and age-group for patients admitted to ICU after suffering a STEMI or NSTEMI.

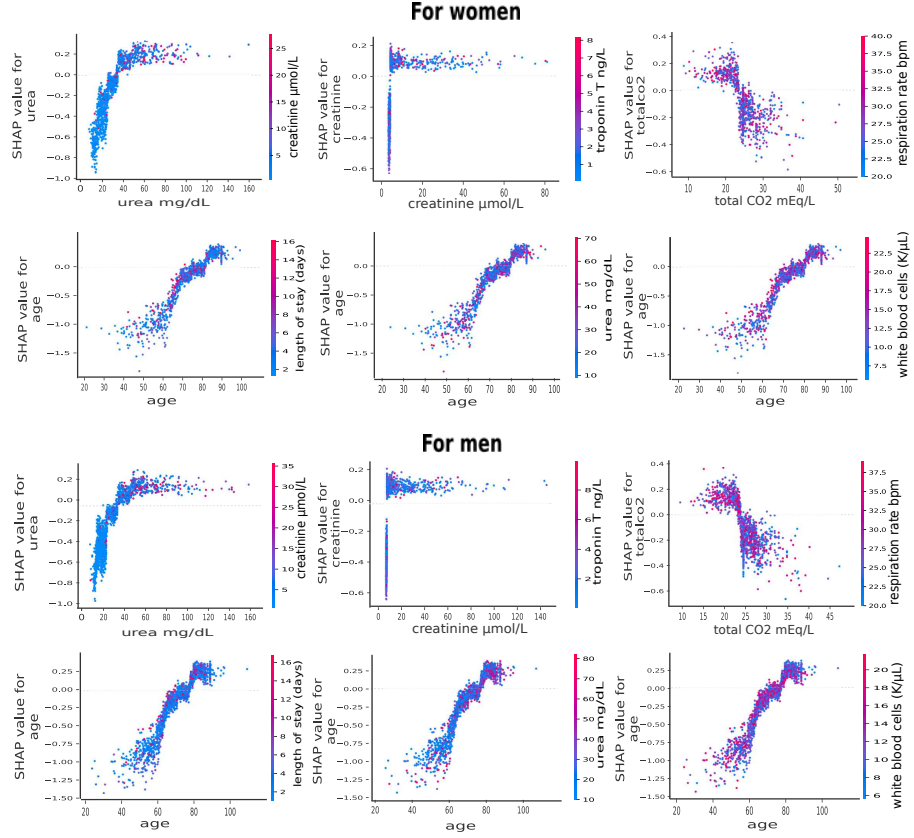


Figure 5: Sex and age-group differences in the top risk markers of patients with NSTEMI

Similarly to this study, Barrett [14] and Choi [31] predicted in-hospital mortality and identified risk markers in patients with myocardial infarction. Barrett evaluated several machine learning methods and found that Logistic Model Trees and Simple Logistic models trained on combined data (admissions, demographics, treatments, diagnostic, laboratory results, and chart events) achieved an AUC=0.90 and identified sex, age, and ethnicity as risk markers. Instead, Choi presented a logistic regression model trained on six features, which achieved an AUC=0.88 and identified age, Glasgow coma score, and anterior wall infarction as markers. However, these models and the corresponding markers considered the entire spectrum of myocardial infarction as a whole. They do not differentiate markers based on sex or age-group or by type of infarct.

As opposed to previous studies, in this study, we obtained two main results. First, we distinguished risk markers according to sex and age for STEMI and NSTEMI. From the clinical point of view, the distinction of markers by type of ACS is essential because each type of infarction differs in the location and extension of coronary involvement; besides, women and men are biologically different; therefore, they should be treated differently, not as a whole. Moreover, we consider that distinguish markers could help fit the strategies of treatments for each sub-population and improve clinical outcomes. Second, we evidenced that mortality prediction models based on the XGB method can provide more accurate risk estimation than some existing standardized scores, such as GRACE.

We computed a multivariable Cox regression model to compare the identified markers by the SHAP approach. Using the Cox model, we identified the statistically significant markers ($P<0.05$) according to sex and age-group for STEMI and NSTEMI. In Table 4, we showed the top markers identified by the Cox model; then, we compared the p-value against the SHAP values. Overall, for women and men with STEMI, almost all of the risk markers identified using SHAP values are statistically significant markers, such as creatinine, urea nitrogen, anion gap and age (where P -value <0.05). All these variables were identified using the SHAP summary and the SHAP feature importance as predictors of mortality. Particularly, the length of stay was not a relevant marker for SHAP and coincided with the p-value (0.26 and 0.31) for women and men, respectively.

In contrast, for NSTEMI, the length of stay and age are markers statistically significant markers for both sexes. Particularly, for NSTEMI, these were the most important markers found by SHAP values as predictors of mortality. It

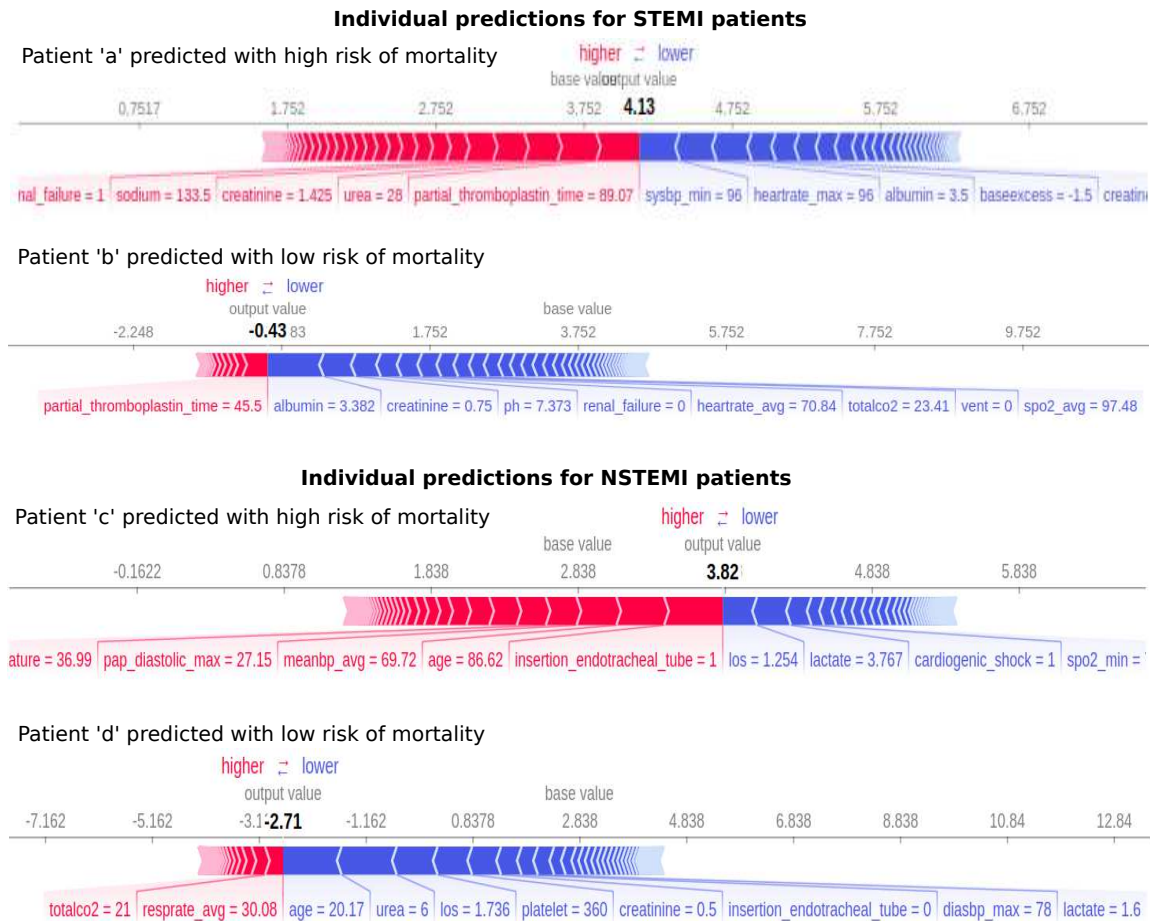


Figure 6: Individual predictions for patients after suffering a STEMI (at the top) or NSTEMI (at the bottom). Each plot shows how each feature contributes to the corresponding model output.

is also worth noting that markers as creatinine, urea, cardiogenic shock, and total CO₂ obtained a low p-value for NSTEMI. Similarly to STEMI, the marker of systolic blood pressure was not relevant to predict mortality, and the p-value obtained was high value (0.94 and 0.61). Interestingly, the marker of lactate obtained a low p-value for women (0.01) and high value for men (0.50); this relationship was also captured for SHAP values (see Figure 3) where women have a higher risk than men by this marker. On the whole, we evidenced that markers identified by SHAP values as predictors of mortality were statistically significant by the Cox model.

Table 4: The top risk markers: a comparative of SHAP values and statistically significant markers by the Cox model

Risk marker	STEMI				NSTEMI			
	Women		Men		Women		Men	
	Average SHAP value	Cox model p-value						
Creatinine	1.46	<0.005*	0.64	<0.005*	0.22	0.03	0.22	0.09
Urea nitrogen	0.44	<0.005*	0.50	<0.005*	0.25	0.02	0.26	0.01
Anion gap	0.33	<0.005*	0.35	<0.005*	0.23	0.18	0.25	0.11
Systolic Blood Pressure	0.61	<0.005*	0.60	<0.005*	0.18	0.94	0.17	0.61
Cardiogenic shock	0.34	<0.005*	0.37	<0.005*	0.11	0.02	0.11	0.01
Heart rate	0.33	0.29	0.32	<0.005*	0.20	0.44	0.17	0.77
Length of stay	0.25	0.26	0.28	0.31	0.57	<0.005*	0.55	<0.005*
total CO2	0.26	<0.005*	0.23	<0.005*	0.16	0.02	0.10	0.06
age	0.25	<0.005*	0.20	0.57	0.38	<0.005*	0.37	<0.005*
lactate	0.23	<0.005*	0.22	<0.005*	0.26	0.01	0.19	0.50

*markers statistically significant ($P < 0.05$)

It is essential to mention that although most of the identified markers describe situations well known in clinical practice, the presence of creatinine, urea, and anion gap for STEMI is often associated with the cardiorenal syndrome, which is not common in infarcted patients. We believe that our approach identified these markers because our cohorts are from

different ICU units, not only the Coronary Care Unit. The ICU unit distribution is as follows: 51% Coronary, 22% Cardiac Surgical Recovery, 21% Medical, 4% Surgical, and 2% Trauma Surgical. We consider that this distribution could contribute to identify markers not common in patients with STEMI and NSTEMI.

This study evaluated several linear and nonlinear machine learning methods and clinical sets for predicting mortality. We observed that models trained with all clinical features extracted achieved a high cross-validated mean AUC compared with models trained with singles set (see table 3). Interestingly, for STEMI, we observed that models trained with laboratory results and complications sets achieved a good performance (AUC=0.87 and AUC=0.81). We believe these results are because both groups contain critical clinical features that contributed to predicting mortality, such as creatinine, urea, anion gap (lab features), and cardiogenic shock and renal failure (complications features). In contrast to NSTEMI, the models trained with procedures and laboratory results achieved a good performance (AUC=0.78 and AUC=0.76). Similarly to STEMI, we believe that both sets contain critical features that increase the probability of death, such as, insertion of endotracheal tube and ventilation (procedures features) and urea and anion gap (lab features). On the other hand, we observed that to train models only with demographic and hemodynamic features achieved the lowest results (AUC under 0.65) for STEMI and NSTEMI. Although the AUC was low for demographic data, it is important to mention that this set contains relevant data, such as age and sex, identified as critical predictors of mortality.

Finally, our findings revealed that machine learning models could help in the identification of risk markers by sex and age-group for sub-populations of patients with cardiovascular diseases. We believe that these identified markers can mark a difference in the definition of treatment plans for each sub-population, improving clinical outcomes.

5 Limitations

We identified the following limitations of our work. First, the EHR extracted from the MIMIC-III database corresponds to patients admitted to different ICUs; hence the identified markers could reflect this bias. We consider that the extraction of EHR from databases of coronary care units could identify more specific markers. Second, we studied a small population of patients (4,119), and the rate of mortality was 8.44%, which could result in overfitting. To alleviate this issue, we measured the AUC-ROC and used Repeated Stratified K-Fold Cross-Validation to assess each model's performance. Also, we consider that increasing the population could improve the model's performance and identify better markers. Another limitation was the selection and characterization of features. For instance, we extracted the minimum, maximum, and average values of the measurements of laboratory, blood gas, hemodynamic, and vital signs. Future works could leverage the use of all the measures captured for each of these features as well as explore feature selection strategies.

6 Conclusions

Using machine learning models and EHR, we identified markers clinically meaningful as predictors of mortality according to sex and age-group for patients admitted to the ICU after a STEMI or NSTEMI. We found the models based on XGB achieved the best performance for STEMI (AUC=0.92) and NSTEMI (AUC=0.87) compared with logistic regression, support vector machine, and random forest.

Then, we used an interpretability approach for identifying the markers that increase the in-hospital mortality for each sub-population. We found that the top markers that increase the risk of mortality for women and men after suffering a STEMI are: the presence of hyponatremia, tachycardia, and metabolic acidosis. More specific markers for women are acute kidney failure, high troponin levels, and age>75 years, while for men are chronic kidney failure, high pulmonary artery pressure, and age>70 years. In contrast, the identified top markers for both sexes after suffering a NSTEMI are: advanced age, extended hospital stays, and intubation procedures. The specific markers for women are low creatinine levels and age>60 years, whilst, for men are damage to the left atrium and age>70 years. Overall, we identified that women have a high risk of dying younger than men after suffering an NSTEMI, even after a STEMI. Likewise, the women have a higher risk of death after an NSTEMI and lower risk of death after a STEMI. Besides, we identified that men have a higher risk of death for both diagnoses after 70 years.

We compared the identified markers by SHAP approach with a Cox model and found that the features are statistically significant; hence the comparison showed that it is possible to find meaningful markers as predictors of mortality. Finally, the markers were evaluated by clinical experts, and they concluded that identified markers are coherent, comparable, and consistent with the clinical routine.

Our study provides further evidence that machine learning applied to cardiovascular diseases could accelerate markers discovery and the development of auxiliary tools to make clinical decisions. Moreover, we consider that the distinction

of markers for each sub-populations could contribute to fitting the treatment strategies to reduce risk and improve the clinical outcomes.

References

- [1] Carmen Mate Redondo, María Cristo Rodríguez-Pérez, Santiago Domínguez Coello, Arturo J. Pedrero García, Itahisa Marcelino Rodríguez, Francisco J. Cuevas Fernández, Delia Almeida González, Buenaventura Brito Díaz, Marcos Rodríguez Esteban, and Antonio Cabrera de León. Hospital Mortality in 415 798 AMI Patients: 4 Years Earlier in the Canary Islands Than in the Rest of Spain. *Revista Española de Cardiología (English Edition)*, 72(6):466–472, June 2019. Publisher: Elsevier.
- [2] J. Tamargo, G. Rosano, T. Walther, J. Duarte, A. Niessner, J. C. Kaski, C. Ceconi, H. Drexel, K. Kjeldsen, G. Savarese, C. Torp-Pedersen, D. Atar, B. S. Lewis, and S. Agewall. Gender differences in the effects of cardiovascular drugs. *European Heart Journal. Cardiovascular Pharmacotherapy*, 3(3):163–182, 2017.
- [3] Cecilia Linde, Maria Grazia Bongiorni, Ulrika Birgersdotter-Green, Anne B. Curtis, Isabel Deisenhofer, Tetsushi Furokawa, Anne M. Gillis, Kristina H. Haugaa, Gregory Y. H. Lip, Isabelle Van Gelder, Marek Malik, Jeannie Poole, Tatjana Potpara, Irina Savelieva, Andrea Sarkozy, ESC Scientific Document Group, Laurent Fauchier, Valentina Kutyifa, Sabine Ernst, Estelle Gandjbakhch, Eloi Marijon, Barbara Casadei, Yi-Jen Chen, Janice Swampillai, Jodie Hurwitz, and Niraj Varma. Sex differences in cardiac arrhythmia: a consensus document of the European Heart Rhythm Association, endorsed by the Heart Rhythm Society and Asia Pacific Heart Rhythm Society. *EP Europace*, 20(10):1565–1565ao, October 2018. Publisher: Oxford Academic.
- [4] Cosme García-García, Lluís Molina, Isaac Subirana, Joan Sala, Jordi Bruguera, Fernando Arós, Miquel Fiol, Jordi Serra, Jaume Marrugat, and Roberto Elosua. Diferencias en función del sexo en las características clínicas, tratamiento y mortalidad a 28 días y 7 años de un primer infarto agudo de miocardio. Estudio RESCATE II. *Revista Española de Cardiología*, 67(1):28–35, January 2014. Publisher: Elsevier.
- [5] Luis Rodriguez-Padial, Cristina Fernández-Pérez, José L. Bernal, Manuel Anguita, Antonia Sambola, Antonio Fernández-Ortiz, and Francisco J. Elola. Differences in in-hospital mortality after STEMI versus NSTEMI by sex. Eleven-year trend in the Spanish National Health Service. *Revista Española de Cardiología (English Edition)*, 2020. Publisher: Elsevier.
- [6] Takeo Onose, Yasuhiko Sakata, Kotaro Nochioka, Masanobu Miura, Takeshi Yamauchi, Kanako Tsuji, Ruri Abe, Takuya Oikawa, Shintaro Kasahara, Masayuki Sato, Takashi Shiroto, Satoshi Miyata, Jun Takahashi, and Hiroaki Shimokawa. Sex differences in post-traumatic stress disorder in cardiovascular patients after the Great East Japan Earthquake: a report from the CHART-2 Study. *European Heart Journal - Quality of Care and Clinical Outcomes*, 3(3):224–233, July 2017. Publisher: Oxford Academic.
- [7] Jim W. Cheung, Edward P. Cheng, Wu, Ilhwan Yeo, Paul J. Christos, Hooman Kamel, Steven M. Markowitz, Christopher F. Liu, George Thomas, James E. Ip, Bruce B. Lerman, and Luke K. Kim. Sex-based differences in outcomes, 30-day readmissions, and costs following catheter ablation of atrial fibrillation: the United States Nationwide Readmissions Database 2010–14. *European Heart Journal*, 40(36):3035–3043, September 2019. Publisher: Oxford Academic.
- [8] Marieke T. Blom, Iris Oving, Jocelyn Berdowski, Irene G. M. van Valkengoed, Abdenasser Bardai, and Hanno L. Tan. Women have lower chances than men to be resuscitated and survive out-of-hospital cardiac arrest. *European Heart Journal*, 40(47):3824–3834, December 2019. Publisher: Oxford Academic.
- [9] Chris Wilkinson, Owen Bebb, Tatendashe B. Dondo, Theresa Munyombwe, Barbara Casadei, Sarah Clarke, François Schiele, Adam Timmis, Marlous Hall, and Chris P. Gale. Sex differences in quality indicator attainment for myocardial infarction: a nationwide cohort study. *Heart*, 105(7):516–523, April 2019. Publisher: BMJ Publishing Group Ltd and British Cardiovascular Society Section: Coronary artery disease.
- [10] Elliott M. Antman, Marc Cohen, Peter J. L. M. Bernink, Carolyn H. McCabe, Thomas Horacek, Gary Papuchis, Branco Mautner, Ramon Corbalan, David Radley, and Eugene Braunwald. The TIMI Risk Score for Unstable Angina/Non-ST Elevation MI: A Method for Prognostication and Therapeutic Decision Making. *JAMA*, 284(7):835–842, August 2000.
- [11] Pedro de Araújo Gonçalves, Jorge Ferreira, Carlos Aguiar, and Ricardo Seabra-Gomes. TIMI, PURSUIT, and GRACE risk scores: sustained prognostic value and interaction with revascularization in NSTE-ACS. *European Heart Journal*, 26(9):865–872, May 2005.
- [12] Keith Fox, Omar H. Dabbous, Robert J. Goldberg, Karen S. Pieper, Kim A. Eagle, Frans Van de Werf, Alvaro Avezum, Shaun G. Goodman, Marcus D. Flather, Frederick A. Anderson, and Christopher B. Granger. Prediction

of risk of death and myocardial infarction in the six months after presentation with acute coronary syndrome: prospective multinational observational study (GRACE). *BMJ*, 333(7578):1091, November 2006.

[13] Hrayr Harutyunyan, Hrant Khachatrian, David C Kale, Greg Ver Steeg, and Aram Galstyan. Multitask learning and benchmarking with clinical time series data. *Scientific Data*, 6:96, June 2019.

[14] Laura A. Barrett, Seyedeh Neelufar Payrovnaziri, Jiang Bian, and Zhe He. Building Computational Models to Predict One-Year Mortality in ICU Patients with Acute Myocardial Infarction and Post Myocardial Infarction Syndrome. *AMIA Joint Summits on Translational Science proceedings*, pages 407–416, 2019.

[15] Harry Hemingway, Gene S. Feder, Natalie K. Fitzpatrick, Spiros Denaxas, Anoop D. Shah, and Adam D. Timmis. *Using nationwide 'big data' from linked electronic health records to help improve outcomes in cardiovascular diseases: 33 studies using methods from epidemiology, informatics, economics and social science in the Clinical disease research using LInked Bespoke studies and Electronic health Records (CALIBER) programme*. Programme Grants for Applied Research. NIHR Journals Library, Southampton (UK), 2017.

[16] Peter C Austin, Douglas S Lee, Ewout W Steyerberg, and Jack V Tu. Regression trees for predicting mortality in patients with cardiovascular disease: What improvement is achieved by using ensemble-based methods? *Biometrical Journal. Biometrische Zeitschrift*, 54(5):657–673, September 2012.

[17] Robert L. McNamara, Kevin F. Kennedy, David J. Cohen, Deborah B. Diercks, Mauro Moscucci, Stephen Ramee, Tracy Y. Wang, Traci Connolly, and John A. Spertus. Predicting In-Hospital Mortality in Patients With Acute Myocardial Infarction. *Journal of the American College of Cardiology*, 68(6):626–635, August 2016.

[18] Liwei Chen, Ling Han, and Jingguang Luo. Risk Factors for Predicting Mortality among Old Patients with Acute Myocardial Infarction during Hospitalization. *The Heart Surgery Forum*, 22(2):E165–E169, 2019.

[19] Alistair E. W. Johnson, Tom J. Pollard, Lu Shen, Li-wei H. Lehman, Mengling Feng, Mohammad Ghassemi, Benjamin Moody, Peter Szolovits, Leo Anthony Celi, and Roger G. Mark. MIMIC-III, a freely accessible critical care database. *Scientific Data*, 3:160035, May 2016.

[20] Robert Jakob. Disease Classification. In Stella R. Quah, editor, *International Encyclopedia of Public Health (Second Edition)*, pages 332–337. Academic Press, Oxford, January 2017.

[21] Partho P. Sengupta, Sirish Shrestha, Béatrice Berthon, Emmanuel Messas, Erwan Donal, Geoffrey H. Tison, James K. Min, Jan D'hooge, Jens-Uwe Voigt, Joel Dudley, Johan W. Verjans, Khader Shameer, Kipp Johnson, Lasse Lovstakken, Mahdi Tabassian, Marco Piccirilli, Mathieu Pernot, Naveena Yanamala, Nicolas Duchateau, Nobuyuki Kagiyama, Olivier Bernard, Piotr Slomka, Rahul Deo, and Rima Arnaout. Proposed Requirements for Cardiovascular Imaging-Related Machine Learning Evaluation (PRIME): A Checklist: Reviewed by the American College of Cardiology Healthcare Innovation Council. *JACC: Cardiovascular Imaging*, 13(9):2017–2035, September 2020.

[22] Fabian Pedregosa, Gaël Varoquaux, Alexandre Gramfort, Vincent Michel, Bertrand Thirion, Olivier Grisel, Mathieu Blondel, Peter Prettenhofer, Ron Weiss, Vincent Dubourg, Jake Vanderplas, Alexandre Passos, David Cournapeau, Matthieu Brucher, Matthieu Perrot, and Edouard Duchesnay. Scikit-learn: Machine Learning in Python. *Journal of Machine Learning Research*, 12:2825–2830, October 2011.

[23] Tianqi Chen and Carlos Guestrin. XGBoost: A Scalable Tree Boosting System. *Proceedings of the 22nd ACM SIGKDD International Conference on Knowledge Discovery and Data Mining*, pages 785–794, August 2016. arXiv: 1603.02754.

[24] Christopher B. Granger, Robert J. Goldberg, Omar Dabbous, Karen S. Pieper, Kim A. Eagle, Christopher P. Cannon, Frans Van de Werf, Alvaro Avezum, Shaun G. Goodman, Marcus D. Flather, Keith A. A. Fox, and for the Global Registry of Acute Coronary Events Investigators. Predictors of Hospital Mortality in the Global Registry of Acute Coronary Events. *Archives of Internal Medicine*, 163(19):2345–2353, October 2003. Publisher: American Medical Association.

[25] Scott M Lundberg and Su-In Lee. A Unified Approach to Interpreting Model Predictions. In I. Guyon, U. V. Luxburg, S. Bengio, H. Wallach, R. Fergus, S. Vishwanathan, and R. Garnett, editors, *Advances in Neural Information Processing Systems 30*, pages 4765–4774. Curran Associates, Inc., 2017.

[26] Scott M Lundberg, Gabriel Erion, Hugh Chen, Alex DeGrave, Jordan M Prutkin, Bala Nair, Ronit Katz, Jonathan Himmelfarb, Nisha Bansal, and Su-In Lee. From local explanations to global understanding with explainable AI for trees. *Nature Machine Intelligence*, 2, 2020.

[27] Scott M Lundberg, Bala Nair, Monica S Avilalala, Mayumi Horibe, Michael J Eisses, Trevor Adams, David E Liston, Daniel King-Wai Low, Shu-Fang Newman, Jerry Kim, and Su-In Lee. Explainable machine-learning predictions for the prevention of hypoxaemia during surgery. *Nature Biomedical Engineering*, 2, October 2018.

[28] Christoph Molnar. *Interpretable machine learning*. Lulu, 2019.
<https://christophm.github.io/interpretable-ml-book/>.

[29] Scott Lundberg. slundberg/shap, October 2020. original-date: 2016-11-22T19:17:08Z.

[30] Gabriela Borrayo-Sánchez, Martín Rosas-Peralta, Erick Ramírez-Arias, Guillermo Saturno-Chiu, Joel Estrada-Gallegos, Rodolfo Parra-Michel, Hugo R. Hernandez-García, Ernesto A. Ayala-López, Rafael Barraza-Felix, Andrés García-Rincón, Débora Adalid-Arellano, Guillermo Careaga-Reyna, José L. Lázaro-Castillo, Lidia E. Betancourt-Hernández, Rocío Camacho-Casillas, Martha Hernández-Gonzalez, Germán Celis-Quintal, Beatriz Villegas-González, Marco Hernández-Carrillo, Zaria M. Benitez Arechiga, Abelardo Flores-Morales, and Ana C. Sepúlveda-Vildosola. STEMI and NSTEMI: Real-world Study in Mexico (RENASCA). *Archives of Medical Research*, 49(8):609–619, November 2018.

[31] Ki Hong Choi, Jeong Hoon Yang, Taek Kyu Park, Joo Myung Lee, Young Bin Song, Joo-Yong Hahn, Seung-Hyuk Choi, Jin-Ho Choi, Yang Hyun Cho, Kiick Sung, Keumhee Carriere, Joonghyun Ahn, and Hyeon-Cheol Gwon. Risk Prediction Model of In-hospital Mortality in Patients With Myocardial Infarction Treated With Venoarterial Extracorporeal Membrane Oxygenation. *Revista Espanola De Cardiologia (English Ed.)*, 72(9):724–731, September 2019.

Risk markers by sex and age group for in-hospital mortality in patients with STEMI or NSTEMI: an approach based on machine learning
Supplementary Material

Appendix 1: ICD-9 codes used to identify STEMI and NSTEMI patients

ICD-9 code	Description
41000	Acute myocardial infarction of anterolateral wall, episode of care unspecified
41001	Acute myocardial infarction of anterolateral wall, initial episode of care
41002	Acute myocardial infarction of anterolateral wall, subsequent episode of care
41010	Acute myocardial infarction of other anterior wall, episode of care unspecified
41011	Acute myocardial infarction of other anterior wall, initial episode of care
41012	Acute myocardial infarction of other anterior wall, subsequent episode of care
41020	Acute myocardial infarction of inferolateral wall, episode of care unspecified
41021	Acute myocardial infarction of inferolateral wall, initial episode of care
41022	Acute myocardial infarction of inferolateral wall, subsequent episode of care
41030	Acute myocardial infarction of inferoposterior wall, episode of care unspecified
41031	Acute myocardial infarction of inferoposterior wall, initial episode of care
41032	Acute myocardial infarction of inferoposterior wall, subsequent episode of care
41040	Acute myocardial infarction of other inferior wall, episode of care unspecified
41041	Acute myocardial infarction of other inferior wall, initial episode of care
41042	Acute myocardial infarction of other inferior wall, subsequent episode of care
41050	Acute myocardial infarction of other lateral wall, episode of care unspecified
41051	Acute myocardial infarction of other lateral wall, initial episode of care
41052	Acute myocardial infarction of other lateral wall, subsequent episode of care
41080	Acute myocardial infarction of other specified sites, episode of care unspecified
41081	Acute myocardial infarction of other specified sites, initial episode of care
41082	Acute myocardial infarction of other specified sites, subsequent episode of care
41090	Acute myocardial infarction of unspecified site, episode of care unspecified
41091	Acute myocardial infarction of unspecified site, initial episode of care
41092	Acute myocardial infarction of unspecified site, subsequent episode of care
4110	Postmyocardial infarction syndrome
4111	Intermediate coronary syndrome
41070	Subendocardial infarction, episode of care unspecified
41071	Subendocardial infarction, initial episode of care
41072	Subendocardial infarction, subsequent episode of care

Appendix 2: STEMI

In this table, we presented the performance for all the trained models using single and combined clinical sets for STEMI.

Model	No. features	Mean cross-validation score	Standard deviation
XGB_combined	191	0.893816189058472	0.034291194517088
LR_combined	191	0.889830011329079	0.035487843516452
GB_lab	40	0.872066152151451	0.039471285805943
LightGB_combined	191	0.869839540733491	0.041827726911116
XGB_lab	40	0.868903978454382	0.039892169383106
SGD_combined	191	0.862313850592425	0.036416478941302
LightGB_lab	40	0.849007884093622	0.040928989444466
SVM_combined	191	0.840255347294198	0.04291182609006
LR_lab	40	0.83742575364109	0.049718154283258
RF_combined	191	0.830598257915994	0.053620248894805
SVM_lab	40	0.802304166526627	0.057467784214112
LR_complications	41	0.802026611370111	0.056397162611587
SGD_lab	40	0.801044765726901	0.056182509299953

XGB_complications	41	0.800015420834697	0.057756450828623
RF_lab	40	0.798735733906629	0.049195373551386
LightGB_complications	41	0.791945892181281	0.063600933378978
XGB_blood	14	0.78869298956193	0.068528722196725
GB_complications	41	0.781621432337495	0.071324143232773
GB_blood	14	0.770349289601196	0.075120774915341
SGD_complications	41	0.750304756419763	0.059786761026245
LR_blood	14	0.73719121677793	0.060193907126381
SVM_blood	14	0.736983869331154	0.05978446767701
SGD_blood	14	0.727649059800539	0.066859339156067
SVM_complications	41	0.722123624761376	0.070645848947752
LightGB_treatments	21	0.717949915523837	0.06317598656754
SVM_procedures	20	0.717457532810506	0.054689556207337
LR_vital	20	0.717059495813945	0.071185471284677
LR_treatments	21	0.716801253264866	0.053821558669677
LR_procedures	20	0.715242535147343	0.054851555642323
GB_vital	20	0.713688450654401	0.059681773594215
SGD_treatments	21	0.711986360460488	0.067569939112303
XGB_treatments	21	0.710070860833433	0.060932766417595
RF_procedures	20	0.709561535724097	0.053786323590845
ADA_lab	40	0.709179363711467	0.048115008223283
GB_treatments	21	0.708653086735399	0.06278610530296
XGB_procedures	20	0.706924065416113	0.055022063721465
LightGB_procedures	20	0.704475820331564	0.055947672262326
GB_combined	191	0.704132117742338	0.035348872648272
GB_procedures	20	0.703750342673948	0.057975526461831
XGB_vital	20	0.701770844678266	0.063263962392347
LightGB_blood	14	0.697315342755712	0.08105767101833
SVM_vital	20	0.693376571187613	0.058343337958532
RF_complications	41	0.693353411041027	0.091618874479726
SGD_procedures	20	0.69194207210548	0.078120342760553
SVM_treatments	21	0.688793668411957	0.065443042880563
ADA_procedures	20	0.687718889135245	0.054062388031992
ADA_combined	191	0.687011043053405	0.052484758176538
ADA_treatments	21	0.684712072566466	0.062696663794064
ADA_blood	14	0.68441716874314	0.077789965193842
SGD_vital	20	0.682058044173372	0.09535538662967
LightGB_vital	20	0.677281237736733	0.062028635493069
ADA_complications	41	0.673106489392044	0.089408245092801
RF_blood	14	0.665985215352669	0.085720222363177
RF_treatments	21	0.659455906241778	0.073318559199297
XGB_demo	10	0.63143860207475	0.059552517527299
XGB_hemo	28	0.624607252100309	0.056779094066299
RF_vital	20	0.624378428429732	0.074320684335717
SVM_demo	10	0.615223099824686	0.062722062176418
SVM_hemo	28	0.614906089950557	0.052904520851164
LightGB_demo	10	0.614484487249825	0.067296282328468
ADA_vital	20	0.608688198866035	0.073136003794508
LR_demo	10	0.607483975759531	0.054389033936495
LightGB_hemo	28	0.603214491091774	0.069325639595201
LR_hemo	28	0.601403020552563	0.053786177376484
GB_demo	10	0.595550702616366	0.066147177082359
ADA_hemo	28	0.58960211260137	0.059931964486739
RF_demo	10	0.58478860780606	0.068909110430751
GB_hemo	28	0.584425914958699	0.07066849064477
ADA_demo	10	0.575907227553463	0.06881337676058

SGD_demo	10	0.569147859304162	0.067939413724764
SGD_hemo	28	0.565356645997469	0.091614154708108
RF_hemo	28	0.546355875367329	0.074694377005729

Appendix 3: NSTEMI

In this table, we presented the performance for all the trained models using single and combined clinical sets for NSTEMI.

Model	No. features	Mean cross-validation score	Standard deviation
XGB_combined	201	0.86678755327628	0.020246720644501
GB_combined	201	0.857812446425223	0.020971446959522
LightGB_combined	201	0.839205006416063	0.022009041637981
SVM_nstemi_combined	201	0.836470463661152	0.021451056416349
SGD_nstemi_combined	201	0.808906617019509	0.035369456054207
XGB_procedures	20	0.781257326615681	0.026146134900382
GB_procedures	20	0.780943164607797	0.026515519763606
LightGB_procedures	20	0.777684514454693	0.029591021246854
RF_combined	201	0.776179371522129	0.028581848424834
SVM_procedures	20	0.76965344286829	0.028828679038465
LR_combinedined	201	0.769548879806284	0.017342455490749
GB_lab	40	0.766116585011545	0.026415373183409
XGB_blood	14	0.759343350451666	0.034003583452377
XGB_lab	40	0.758140170849112	0.0270494525828
LR_lab	40	0.753804907680957	0.03238945203092
RF_procedures	20	0.753793961770319	0.031789576556489
LR_complications	52	0.750021471463066	0.033715840501247
GB_complications	52	0.747001315354877	0.037403664538805
XGB_complications	52	0.746857804941324	0.034609605645857
LR_procedures	20	0.745196582775497	0.037936023123591
ADA_procedures	20	0.744210571149597	0.031474311774951
GB_blood	14	0.738748180174341	0.034178417535931
SVM_lab	40	0.737820793353014	0.034834181545523
LightGB_complications	52	0.737782125860069	0.03698589654518
GB_vital	20	0.725613840925588	0.037500035874083
LightGB_lab	40	0.725560852442822	0.024822739836191
SVM_complications	52	0.717575808810337	0.042236750572578
XGB_vital	20	0.71012540362796	0.037740441329553
RF_blood	14	0.707933918950758	0.03464698131686
ADA_combined	201	0.70179912261185	0.036059655281746
RF_complications	52	0.696826842282156	0.040176438480421
SGD_lab	40	0.695887923284628	0.053294113804698
LR_vital	20	0.694550735220221	0.042130121354787
SVM_vital	20	0.69413219442119	0.043722926692678
SGD_procedures	20	0.693231644542303	0.047041512929196
RF_lab	40	0.689755068539975	0.030588647510636
SVM_blood	14	0.684379570894236	0.043419585368106
ADA_complications	52	0.682544724170501	0.036603143293926
LightGB_vital	20	0.68063208874996	0.035276705069886
LR_blood	14	0.67928148051089	0.044715208458671
LightGB_blood	14	0.679060377477382	0.043942507097078
SGD_complications	52	0.671619501390411	0.042950359705742
GB_treatments	21	0.663150116554399	0.040399894266849
ADA_lab	40	0.660880790232145	0.031780061618388
XGB_treatments	21	0.660029274284349	0.042510319556109

ADA_blood	14	0.655735549699285	0.044673342737681
SGD_vital	20	0.648940945880138	0.048671644621299
XGB_hemo	28	0.646494305008963	0.035885611496757
SVM_treatments	21	0.644917986431889	0.040550684650678
LightGB_treatments	21	0.641051761594589	0.04152597194624
GB_hemo	28	0.638064058912853	0.033740716235367
RF_vital	20	0.633017242463813	0.040338405179483
LR_treatments	21	0.630057633631465	0.040352289927359
RF_treatments	21	0.62541868876156	0.047473781371702
LightGB_hemo	28	0.625373741775157	0.039545242233073
SVM_hemo	28	0.611598031696144	0.030806931572668
XGB_demo	10	0.610259569747604	0.037155415274751
SGD_blood	14	0.609290704647416	0.053847047010502
ADA_treatments	21	0.608281857464363	0.041150636522432
SVM_demo	10	0.607936993115682	0.037865468039159
LR_hemo	28	0.606606328912309	0.030683980775259
LightGB_demo	10	0.603265719020366	0.038979729306524
ADA_hemo	28	0.599396639996175	0.033363713484575
RF_hemo	28	0.592364353009964	0.03333648153209
ADA_demo	10	0.589914235380009	0.030087595107553
GB_demo	10	0.589148919690342	0.034677560923515
RF_demo	10	0.588435804092103	0.038669966701145
SGD_hemo	28	0.585498882614644	0.056802742121103
SGD_treatments	21	0.583942443323145	0.041474867709426
ADA_vital	20	0.58240882400745	0.03715797035756
LR_demo	10	0.58213798034178	0.037184876727691
SGD_demo	10	0.536961420608568	0.047665041514286